Preliminary 3D Computational Analysis of the Relationship between Aortic Displacement Force and Direction of Endograft Movement

C. Alberto Figueroa, PhD[1]; Charles A. Taylor, PhD[1, 2]; Victoria Yeh[1]; Allen J. Chiou[1]; Madhu L. Gorrepati[2], MD; Christopher K. Zarins, MD[2]

Departments of [1]Bioengineering and [2]Surgery, Stanford University, Stanford, CA, USA

Presented by C. A. Figueroa at the XXIV Annual Meeting Western Vascular Society, Tucson, AZ, September 20, 2009

Abstract 383 words; Manuscript body: 4046 words

Address for correspondence and reprints: Dr Christopher K. Zarins, Department of Surgery, Clark Center E350A, 318 Campus Drive West, Stanford, California, 94305-5431. E-mail: zarins@stanford.edu.

Supported by: National Institutes of Health/NHLBI grant 2R01 HL64327-05A1

Competition of interests: none

ABSTRACT

Objective:

Endograft migration is usually described as a downward displacement of the endograft with respect to the renal arteries. However, change in endograft position is actually a complex process in three dimensional space. Currently, there are no established techniques to define such positional changes over time. The purpose of this study is to determine whether the direction of aortic endograft movement as observed in follow-up CT scans is related to the directional displacement force acting on the endograft.

Methods:

We quantitated the 3D positional change over time of 5 abdominal endografts by determining the endograft centroid at baseline (post-operative scan) and on follow-up CT scans. The time interval between CT scans for the 5 patients ranged from 8 months to 8 years. We then used 3D image segmentation and computational fluid dynamics (CFD) techniques to quantitate the pulsatile displacement force (in Newtons [N]) acting on the endografts in the post-operative configurations. Finally, we calculated a correlation metric between the direction of the displacement force vector and the endograft movement by computing the cosine of the angle of these two vectors.

Results:

The average 3D movement of the endograft centroid was 18 mm (range 9 mm to 29 mm) with greater movement in patients with longer follow-up times. In all cases, the movement of the

endograft had significant components in all 3 spatial directions: Two of the endografts had the largest component of movement in the transverse direction, whereas 3 endografts had the largest component of movement in the axial direction. The magnitude and orientation of the endograft displacement force varied depending on aortic angulation and hemodynamic conditions. The average magnitude of displacement force for all endografts was 5.8 N (range 3.7 N to 9.5 N). The orientation of displacement force was in general perpendicular to the greatest curvature of the endograft. The average correlation metric, defined as the cosine of the angle between the displacement force and the endograft centroid movement, was 0.38 (range 0.08 to 0.66).

Conclusions:

Computational methods applied to patient-specific post-operative image data can be used to quantitate three-dimensional displacement force and movement of endografts over time. It appears that endograft movement is related to the magnitude and direction of the displacement force acting on aortic endografts. These methods can be used to increase our understanding of clinical endograft migration.

Key words: displacement forces, endograft movement, abdominal aortic aneurysm, angulation and curvature, computational fluid dynamics, patient-specific.

INTRODUCTION

During the past decade endovascular aneurysm repair (EVAR) has become the treatment of choice for patients with abdominal aortic aneurysms. EVAR significantly reduces morbidity and mortality when compared to open repair [1, 2]. However, endografts are prone to late failure due to the loss of positional stability (an event clinically known as endograft migration) resulting from the pulsatile forces of blood flow [3, 4]. Endograft failure may lead to costly secondary procedures, conversion to open repair, aneurysm rupture and death. To date, there has not been a consistent definition of endograft migration. Migration has been variously defined using an arbitrarily selected distance, such as 5 or 10 mm, or in some cases based on the clinical need for a secondary intervention [3, 5, 6]. Previous studies quantifying endograft movement have relied on one-dimensional [3, 7, 8] or two-dimensional [9] techniques. Measurements have included axial or centerline distances from the renal arteries or superior mesenteric artery to the first appearance of the endograft or to the appearance of the complete fabric-stent ring. However, endograft positional change over time is a three-dimensional event and to date, no reports have described endograft movement in quantifiable three-dimensional terms. Quantification of 3D positional changes of the endograft over time is challenging due to the geometric complexity of the endograft, the need to co-register two different images in space, and the non-uniform movement of the device, since some parts of the endograft may experience a significant movement while others remain stationary. In this study, we considered the point given by the centroid of the endograft and tracked this point over time in order to describe the 3D movement of the endograft. Furthermore, we used

previously developed Computational Fluid Dynamics (CFD) tools [14] to determine the 3D displacement forces acting on computer models of aortic endografts built from post-operative CT scan data. This study represents our initial effort to quantitatively relate 3 dimensional positional changes of endografts over time to 3 dimensional displacement forces acting on aortic endografts. Future quantitative studies using these methods may be applied to larger numbers of patients in order to increase our understanding of clinical endograft migration.

METHODS

Patient Population

Five patients with abdominal aortic aneurysms (AAA) who underwent EVAR at our institution and were followed with serial imaging and clinical follow-up data were selected for this study from our aortic aneurysm database which includes more than 500 patients. Informed consent was obtained from each patient prior to surgery, and all follow-up protocols, including imaging, were approved by the Institutional Review Board. The five patients were selected for the purpose of developing the computational methods detailed in this study and each had readily available serial imaging studies of suitable quality. Since the methods of this study are focused on the study of displacement forces and endograft movement, we included 4 patients with clinical evidence of migration. We also included a patient with no evidence of clinical migration during an 8.5 year follow-up. These patients reflect a broad range of aneurysm sizes (5.0 to 8.6 cm), clinical outcomes, and follow-up times, but do not necessarily reflect the population of patients treated with EVAR at our institution. Clinical data included age, gender, height and

weight, pre-operative aneurysm size, post-operative systolic and diastolic blood pressure and heart rate (see Table 1). The baseline CT for each patient was compared to the latest follow-up CT or the last CT scan before a secondary intervention. The time interval between baseline and follow-up imaging varied from 8 months to 8.5 years. The mean time interval between the scans considered was 3.3 years. Figure 1 shows the CT data of the 5 patients corresponding to the post-operative baseline scan (top row) and the latest follow-up scan (bottom row).

3D Endograft Movement Analysis

Post-operative and follow-up CT scans were evaluated using TeraRecon Aquarius Net software (TeraRecon Inc, San Mateo, CA) to generate volume-rendered images of the aneurysm and endograft. The open-source software itk-SNAP [15] was used to generate 3D segmentations and level-sets of models of the aorta and stent-graft. We then used the open-source software SimVascular [16], and in-house software for solid discrete model triangulation of the level-set functions and for finite element mesh generation [17]. Finally, we used the open-source software Paraview (Kitware, Inc. Clifton Park, NY) for visualization of CFD results and measurement of 3D distances. In this work, we characterized the 3D movement of the endograft by tracking the position of the endograft centroid in baseline and follow-up scans and co-registering these two positions in the baseline scan using the center point on the inferior edge of the L3 vertebra as an anatomic landmark. The centroid of the endograft was calculated as the average coordinate of the points that lay on the fabric of the device. The fabric of the endograft was segmented out using the aforementioned software, neglecting supra-renal fixations when present. Figure 2 shows the 3D endograft movement analysis for patient #2 of

the study. The top and middle rows show volume-renderings of the baseline and one year follow-up image data, respectively. The bottom row shows a maximum intensity projection (MIP) of the baseline image data showing the reference point used for 3D co-registration between the two scans (yellow dot), the endograft centroid in the baseline scan (red dot), and the endograft centroid in the one-year follow-up scan (green dot). The distance between the two centroids was used to characterize the 3D movement of the endograft, which has components in the anterior, lateral, and axial directions.

Endograft Displacement Force analysis

Figure 3 depicts the methodology adopted to calculate the displacement force acting on the endografts. Starting with the Computed Tomography Angiography (CTA) data corresponding to the baseline scan of each patient, 3D computer models of the abdominal aorta and endograft were built for each patient using the itk-SNAP segmentation software [15] and our in-house software for solid discrete model triangulation and mesh generation [16,17]. The computer models included data from the supraceliac aorta to the iliac arteries, including the celiac, superior mesenteric, and renal arteries. The models were discretized into finite element meshes with an average size of 2.175 million linear tetrahedral elements (element size 0.76 mm). We then performed computational fluid dynamic (CFD) analyses to simulate pulsatile blood flow and blood pressure using techniques developed by our group [18-21] for patient-specific boundary condition specification to ensure that physiologic levels of pressure are attained in the numerical simulations. Accurate pressure results are critical to obtaining realistic values for the displacement force. We considered patient-specific data for systolic and diastolic

blood pressures recorded at the time of the post-operative scans. This study is based on retrospective patient data and none of the patients included had PC-MRI data. Supraceliac flow was estimated using a population-based study of phase-contrast MRI flow measurements in a large cohort of 36 AAA patients [22]. In that study, linear regression analyses were performed to correlate mean supraceliac and infrarenal flows with different morphometric parameters such as patient height, weight, body surface area and fat-free body mass. The study shows that the best predictor of mean supraceliac and infrarenal flow is body surface area. In this work, we have estimated the supraceliac flow waveform for each patient as a function of their body surface area and their measured post-operative heart rate. Table 1 summarizes the estimated supraceliac mean flow calculated using PC-MRI population data. This data ensured that adequate boundary conditions were derived to represent the post-operative hemodynamic state of each of the patients.

Figure 4 shows the comparison between the pulsatile pressure wave obtained in the CFD analysis of each patient and the measured single values of peak systolic and diastolic pressures obtained at the time of the post-operative scan. The comparison shows that the pulsatile pressure waves obtained in the analysis lie within the limits of the post-operative pressure measurements. The maximum relative error between the computed and measured data for the pressure pulse was less than 3% for all the patients. The peak systolic and diastolic pressure measurements undoubtedly vary over time, impacting the endograft displacement force. However, for simplicity and due to the lack of more detailed pressure history measurements for each patient in this study, we have assumed that the single post-operative values of peak

systolic and diastolic pressure remained constant through the follow-up period for each patient. Once the CFD analysis was completed, we calculated the magnitude and direction of time-varying displacement forces exerted by blood flow on the endografts by integrating the distribution of tractions acting on the fabric of the device. The tractions included the effects of both the pressure and shearing stresses of blood. Blood pressure is several orders of magnitude larger (usually around 10,000 times larger) than the shear stress. This factor, together with the main curvature of the graft, dictates the magnitude and orientation of the displacement force [11,14,24]. Once we computed the 3D endograft movement between the baseline and follow-up scans and the 3D displacement force acting on the baseline configuration, we investigated the correlation between these vectors.

The time for clinical and image data processing, computation, and analysis of the results was approximately 4 weeks per patient.

RESULTS

Patient population

Characteristics of the 5 patients selected for this study are shown in Table 1. Patients included 4 men and 1 woman with a mean age of 76 years. Aneurysm size ranged from 5.0 cm to 8.6 cm (mean 6.3 cm). Four patients had clinical evidence of endograft migration requiring secondary treatments and one patient had no migration or clinical events for 8.5 years after endograft placement. Patient 1 had no endoleak and experienced a decrease in aneurysm size after EVAR.

Imaging studies over 3 years revealed progressive anterior displacement of the endograft in the aneurysm sac with downward displacement of the proximal endograft relative to the renal arteries with no evidence of a type I endoleak. He was electively treated with a proximal extender 3 years and 3 months after initial endograft placement. Patient 2 had a 8.6 cm aneurysm with a short, angulated infrarenal neck. Six months after EVAR there was no endoleak and the aneurysm decreased in size slightly; there was a 9mm anterior movement of the endograft in the aneurysm sac. At one year the patient developed a new onset proximal type I endoleak and was treated with proximal and distal extenders. Patient 3 was treated with a suprarenal endograft and flared iliac limb extenders. Follow-up imaging at 8 months showed aneurysm enlargement and a left iliac type I endoleak. This was treated with coil embolization of the hypogastric artery and extension to the external iliac artery. Subsequent CT scans showed no endoleak with evidence of anterior movement of the endograft in the aneurysm sac. The 8 month CT was used in this analysis. Patient 4 had severe aortic neck angulation and marked aneurysm tortuosity. There was progressive increase in angulation of the aneurysm and endograft over 3 years with no endoleak. A proximal type I endoleak developed at 3.5 years with aneurysm enlargement. Endovascular treatment was not possible and the endoleak was sealed by externally wrapping the aortic neck with a Dacron band. Patient 5 has been clinically well for 8.5 years with no aneurysm or endograft related events. The patient had follow-up imaging on an annual basis and had no endoleak, no migration and marked reduction in aneurysm size from 6.0 cm to 3.4 cm.

3D Movement of endograft centroid between baseline and follow-up scans

Table 2 summarizes the findings for the endograft 3D movement in the 5 patients, calculated as the motion of the centroid between the post-operative and follow-up scans. The average distance moved was 18 mm (range 9 mm to 29 mm). The movement of the centroid was generally larger for patients with longer follow-up intervals. All patients presented significant transverse (antero-lateral plane xy) endograft motion (average 12 mm, range 7 mm to 18 mm). Two endografts had the largest component of movement in the transverse direction, whereas 3 had the largest component of movement in the axial direction (z axis). It is important to note that patient 5 did not experience clinical migration, despite the very significant endograft movement of 14 mm.

Magnitude and direction of Displacement Force vector

Table 2 summarizes the results for the magnitude and 3D components of the displacement force vectors for the 5 patients (given in Newtons) in the anterior (x), lateral (y) and axial (z) directions. The average displacement force magnitude was 5.8 N. The maximum displacement force (9.5 and 5.6 N) corresponded to patients who experienced the earliest signs of endograft movement (patients 2 and 3). The displacement force was in general perpendicular to the greatest curvature of the endograft rather than along the longitudinal centerline axis of the vessel. Patients 1 and 4 had the largest component of the displacement force vector in the axial (z) direction. Conversely, patients 2, 3 and 5 had the largest component of the displacement force vector in the anterior (x) direction. All patients presented significant transverse endograft displacement force (average of 4.5 N). Figure 5 shows anterior and lateral views of the

computed displacement force vector (red arrows in the figure) acting on the post-operative configuration. The relative sizes of the arrows reflect the magnitude of the vectors.

Relationship between 3D aortic Displacement Force and direction of endograft movement

We computed the angle α between the displacement force vector and the movement vector for each patient. Then, we calculated the cosine of the angle α using the formula

$$\cos(\alpha) = \frac{\text{dot(DF, movement)}}{\text{magnitude(DF)} \times \text{magnitude(movement)}} \quad , \qquad (1)$$

where dot(DF, movement) represents the dot product between the displacement force and the movement vectors. This parameter was used as a correlation metric between the displacement force and movement vectors. For instance, if the two vectors were aligned, then cos(α)=1.0, representing a perfect correlation. On the contrary, if the two vectors were perpendicular to each other, then cos(α)=0.0, representing no correlation. Lastly, if the two vectors pointed in opposite directions, then cos(α)=-1.0, implying an inverse correlation between displacement force and movement. Table 2 shows the numerical values of cos(α). The average correlation metric between displacement force and movement vectors was 0.38. This corresponds to an average angle between the displacement force and movement vectors of α = 67 degrees. With the exception of patient 3 (who showed a very small correlation between displacement force and displacement vectors), the correlation between the orientation of the post-operative displacement force vector and the movement vector was rather high for the patients with shorter follow-up intervals. Thus, patients with a time interval of less than 3.5 years between scans (patients 1, 2, and 4) had an average correlation metric of 0.54, corresponding to an angle

between displacement force and movement vectors of α =57 degrees. Figure 5 shows anterior and lateral views of the computed displacement force vector (red arrow) and measured movement vector (yellow arrow) on the post-operative endograft configuration. The size of the arrows reflects the magnitude of the vectors.

DISCUSSION

Endograft movement evaluation

Clinical studies of endograft migration have focused on factors such as aortic neck length, diameter and angulation, proximal and distal endograft fixation and features of endograft design [3-8]. Most studies have defined migration in terms of downward displacement of the endograft with respect to a fixed arterial reference point such as the renal arteries or superior mesenteric artery. However, change in endograft position over time is a complex process in 3D space. Devices can move laterally within the aneurysm sac, thus affecting the position of the top of the endograft [9]. Movement within the aneurysm sac can be in the anterior, lateral and axial directions depending on endograft fixation characteristics, tortuosity of the anatomy, and the magnitude of the loads exerted by blood flow on the device. This work represents our first effort to characterize endograft displacement in 3D space over time using the centroid of the endograft as a surrogate for the movement of the entire device. In order to avoid confusion with the large literature related to endograft 'migration', we have restricted ourselves to using the term 'movement' when referring to positional change. Quantification of 3D positional changes of the endograft over time is challenging due to geometric complexity of the

endograft, the need to co-register two different images in space, and non-uniform device movement. We quantified positional changes of the endograft centroid relative to the fixed reference point of the inferior edge of the L3 vertebra. It should be noted that the endograft centroid may be outside the endograft in cases of high curvature. Given the differences between our measurement technique and traditional 2D-based techniques, the definition of movement or migration in this study may differ from what is generally understood.

Endograft displacement force evaluation

In this work, we have performed CFD simulations in geometrically-accurate 3D patient-specific models of AAA stent-grafts, using boundary conditions that faithfully represented the patient post-operative hemodynamic conditions, in an attempt to estimate the magnitude and orientation of the forces experienced by the device over the cardiac cycle. Previous experimental and computational studies have evaluated the displacement forces acting on different devices, which in general are designed to resist downwards displacement using a variety of fixation mechanisms. Most of these studies have considered greatly idealized conditions regarding the geometries of the aneurysm and stent-graft, often neglecting curvatures in the anterior and lateral directions [10-13]. As a result, the reported forces have been assumed to act primarily in the downwards (caudal) direction of blood flow. In this study, we found that the orientation of displacement force was in general perpendicular to the greatest curvature of the endograft. The magnitude and orientation of the endograft displacement force varied depending on aortic angulation and hemodynamic conditions.

285 Blood pressure changes have a direct bearing on displacement force: the larger the pressure,
286 keeping all remaining factors such as endograft size, length, tortuosity, etc. unchanged, the
287 larger the displacement force [11,24]. Displacement force is also related to the size of the
288 endograft: previous computational studies [11,24] show that the larger the size of the
289 endograft, keeping all remaining factors such as blood pressure, endograft length, tortuosity,
290 etc. unchanged, the larger the displacement force. Likewise, the inner surface of the endograft
291 (i.e., nature of fabric, suture points between stent and graft, etc.) may be of influence in the
292 overall displacement force. In this work, we have segmented the luminal surface of the
293 endograft using sub-millimeter resolution direct-3D techniques that enable the reconstruction
294 of the stents superimposed on the graft surface. The fixation response of the endograft, also
295 known as fixation force, depends on the specific fixation system (i.e., radial force, supra-renal
296 fixation, presence of hooks and barbs), the fixation length and the presence of longitudinal
297 columnar force wires. In this work, we have assumed that the endograft and aneurysm walls
298 are rigid and that there is a smooth connection between them. Future work will improve upon
299 what has been presented here to investigate the specific endograft fixation response as a
300 function of the parameters mentioned above.

301 Pre-implantation aortic morphology (i.e. proximal fixation length, neck angle, etc.) will
302 undoubtedly affect both the displacement force experienced by the graft and its fixation
303 response. However, these considerations fall outside the scope of the current study. In future
304 investigations, we will investigate the correlation of endograft displacement forces with pre-
305 operative aneurysm size, aortic neck tortuosity, etc. Furthermore, the calculated displacement

force may change if the geometry of the endograft changes significantly as a result of the endograft movement. In some instances it will increase and in others it will decrease. The description of these changes in displacement force over time requires longitudinal studies that compute the force at each available image dataset for the patient. This will be the subject of future study.

Clinical migration and correlation between endograft movement and displacement force

Four of the 5 patients (patients 1, 2, 3, 4) in this study had clinical evidence of migration from 8 months to 3.5 years after EVAR. In 3 cases (patients 1, 2, and 4) the movement of the endograft centroid was correlated to the direction of the displacement force acting on the endograft. In the case of patient 3, the correlation metric between movement and displacement force was small. This patient was treated for a type I left iliac endoleak at 8 months resulting from endograft movement in the lateral direction (see Figure 5). Subsequent follow-up CT scans show that the endograft centroid was moving in the direction of the displacement force. Patient 5 had no clinical migration at 8.5 years after EVAR. Nonetheless, this patient had evidence of movement of the endograft centroid over time. The direction of movement correlated to displacement force direction in late follow-up at 8.5 years.

The discrepancies observed between the direction of movement and direction of displacement force may be due to several factors: First, in this paper we used a simple index (the centroid of the endograft) to track the movement in 3D space of the device. More sophisticated techniques based on 3D rigid and deformable registrations [23] may be used to obtain a description of the movement that is not reduced to the position of the centroid and that can therefore produce

different values for the movement. Second, in order to more accurately predict the displacement force acting on the endograft, one must take the effects of the stiffness of the endograft and surrounding tissues (mural thrombus, plaque, aortic wall, etc.) into account. Different stiffness in different areas will affect the overall response of the stent-graft to the forces exerted by the blood flow. In this analysis, we did not consider the stiffness of surrounding tissue and organs, and modeled the endograft as rigid. Future work will take these features into account and may improve the correlation between the orientation of the computed displacement force and the measured endograft movement. Furthermore, in the displacement force analysis, we have assumed that pressure in the aneurysm sac after endograft deployment is zero: this is not the case in patients who have endoleaks after endovascular aneurysm repair. Although the small number of patients analyzed limits any definite clinical conclusions, the results indicate that there might be a correlation between the post-operative displacement force and the early direction of endograft movement. Understanding the correlation between endograft displacement forces and movement is a critical aspect that can be used to improve endograft design and performance.

In this study, we have included patients with and without endograft clinical migration. The patients with clinical migration had movement of the endograft. Interestingly, the patient who had no clinical migration over 8.5 years also had movement of the endograft. This suggests that the DF acts on the endograft and whether clinical migration occurs or does not occur depends on more than one factor (i.e. DF alone does not determine migration). Furthermore, from a physical standpoint, the displacement force exists for all grafts since these forces are the result

of the actions of blood flow (pressure, and wall shear stress) and the geometry (length, angulation, diameter) of the graft. Therefore, even grafts that do not experience movement are also subject to displacement forces (which may be arguably smaller than the cases presented here). For these stable grafts, the fixation forces developed in the proximal and distal fixation areas, and the external tissue of the aneurysm sac may provide large levels of support that help keep the endograft in place. This topic will be the subject of future studies.

The analysis presented here is just a first step and needs to be expanded to investigate the effects of aforementioned factors that may influence both the method of defining endograft movement and the analysis of magnitude and direction of displacement force. However, it will be important to ensure that enhancing the complexity of displacement force and movement characterization is done in a way such that computational requirements can still be performed in a clinically-relevant time frame.

Conclusions:

This represents the first quantitative study relating three-dimensional displacement force acting on aortic endografts to 3D positional changes of the endograft over time. The orientation of displacement force is in general perpendicular to the greatest curvature of the endograft rather than along the longitudinal centerline axis of the aorta. Endograft movement appears to be related to the magnitude and direction of the displacement force. Patient-specific computational models can be used to increase our understanding of clinical endograft migration.

REFERENCES

1. Greenhalgh RM, Brown LC, Kwong GPS, Powell JT, Thompson SG: Comparison of endovascular aneurysm repair with open repair in patients with abdominal aortic aneurysm (EVAR trial 1), 30-day operative mortality results: randomised controlled trial. Lancet 2004; 364(9437): 843-48.

2. Prinssen M, Buskens E, Blankensteijn JD: Quality of life after endovascular and open AAA repair: Results of a randomized trial. European Journal of Vascular Surgery 2004; 27(2): 121-127.

3. Zarins CK, Bloch DA, Crabtree T, Matsumoto AH, White RA, Fogarty TJ: Stent graft migration after endovascular aneurysm repair: importance of proximal fixation. Journal of Vascular Surgery 2003; 38(6): 1264-72.

4. Zarins CK: Stent-graft migration: how do we know when we have it and what is its significance? Journal of Endovascular Therapy 2004; 11(4): 364-5.

5. Matsumura JS, Brewster DC, Makaroun MS, Naftel DC: A multicenter controlled clinical trial of open versus endovascular treatment of abdominal aortic aneurysm. Journal of Vascular Surgery 2003; 37(2): 262-271.

6. Sternbergh WC, Money SR, Greenberg RK, Chuter TAM: Influence of endograft oversizing on device migration, endoleak, aneurysm shrinkage, and aortic neck dilation. Journal of Vascular Surgery 2004; 39(1): 20-26.

7. Resch T, Ivancev K, Brunkwall J, Nyman U, Malina M, Lindblad B: Distal migration of stent-grafts after endovascular repair of abdominal aortic aneurysms. Journal of Vascular and Interventional Radiology 1999; 10(3): 257-264.

8. Benharash P, Lee JT, Abilez OJ, Crabtree T, Bloch DA, Zarins CK: Iliac fixation inhibits migration of both suprarenal and infrarenal aortic endografts. Journal of Vascular Surgery 2007; 45(2): 250-257.

9. Rafii BY, Abilez OJ, Benharash P, Zarins CK: Lateral movement of endografts within the aneurysm sac is an indicator of stent-graft instability. Journal of Endovascular Therapy 2008; 15(3): 335-343.

10. Morris L, Delassus P, Walsh M, McGloughlin T: A mathematical model to predict the in vivo pulsatile drag forces acting on bifurcated stent grafts used in endovascular treatment of abdominal aortic aneurysms (AAA). Journal of Biomechanics 2004; 37(7): 1087-1095.

11. Li Z, Kleinstreuer C, Farber M: Computational analysis of biomechanical contributors to possible endovascular graft failure. Biomechanics and Modeling in Mechanobiology 2005; 4(4): 221-34.

12. Howell B, Kim T, Cheer A, Dwyer H, Saloner D, Chuter T: Computational Fluid Dynamics within bifurcated abdominal aortic stent-grafts. Journal of Endovascular Therapy 2007; 14: 138-43.

13. Molony DS, Callanan A, Morris LG, Doyle BJ, Walsh MT, TM M: Geometrical enhancements for abdominal aortic stent-grafts. Journal of Endovascular Therapy 2008; 15: 518-29.

14. Figueroa CA, Taylor CA, Chiou AJ, Yeh V, Zarins CK: Effect of Curvature on Displacement Forces Acting on Aortic Endografts: a three dimensional computational analysis. Journal of Endovascular Therapy 2009; 16:284-294.

15. Yushkevich PA, Piven J, Hazlett HC, Smith RG, Ho S, Gee JC, Gerig G: User-guided 3D active contour segmentation of anatomical structures: Significantly improved efficiency and reliability. Neuroimage 2006; 31(3): 1116-28.

16. Cardiovascular Modeling and Simulation Application. http://wiki.simtk.org/simvascular/SimVascular.

17. Xiong G, Figueroa CA, Xiao N, Taylor CA: Simulation of blood flow in deformable arteries using subject-specific geometry and variable vessel wall properties. Proceedings of the ASME Summer Bioengineering Conference, 2009. Lake Tahoe, Ca.

18. Taylor CA, Hughes TJR, Zarins CK: Finite element modeling of blood flow in arteries. Computer Methods in Applied Mechanics and Engineering 1998; 158(1-2): 155-196.

19. Vignon-Clementel IE, Figueroa CA, Jansen KE, Taylor CA: Outflow boundary conditions for three-dimensional finite element modeling of blood flow and pressure in arteries. Computer Methods in Applied Mechanics and Engineering 2006; 195(29-32): 3776-3796.

20. Figueroa CA, Vignon-Clementel IE, Jansen KE, Hughes TJR, Taylor CA: A coupled momentum method for modeling blood flow in three-dimensional deformable arteries. Computer Methods in Applied Mechanics and Engineering 2006; 195(41-43): 5685-5706.

21. Kim HJ, Figueroa CA, Hughes TJR, Jansen KE, Taylor CA: Augmented Lagrangian method for constraining the shape of velocity profiles at outlet boundaries for three-dimensional finite element simulations of blood flow. Computer Methods in Applied Mechanics and Engineering 2009; 198: 3551-3566.

22. Les AS, Yeung JJ, Young PM, Herfkens RJ, Dalman RL, Taylor CA: Volumetric Flow at the Supraceliac and Infrarenal Levels In Patients with Abdominal Aortic Aneurysm: Waveforms and Allometric Scaling Relationships. Proceedings of the ASME Summer Bioengineering Conference, 2009. Lake Tahoe, CA.

23. Hill DLG, Batchelor PG, Holden M, Hawkes DJ: Medical Image Registration. Physics in Medicine and Biology 2001; 46(3): R41-R45.

24. Figueroa CA, Taylor CA, Chiou AJ, Yeh V, Zarins CK: Magnitude and direction of pulsatile displacement forces acting on thoracic aortic endografts. Journal of Endovascular Therapy 2009, 16: 350-358.

Figure 1

Click here to download high resolution image

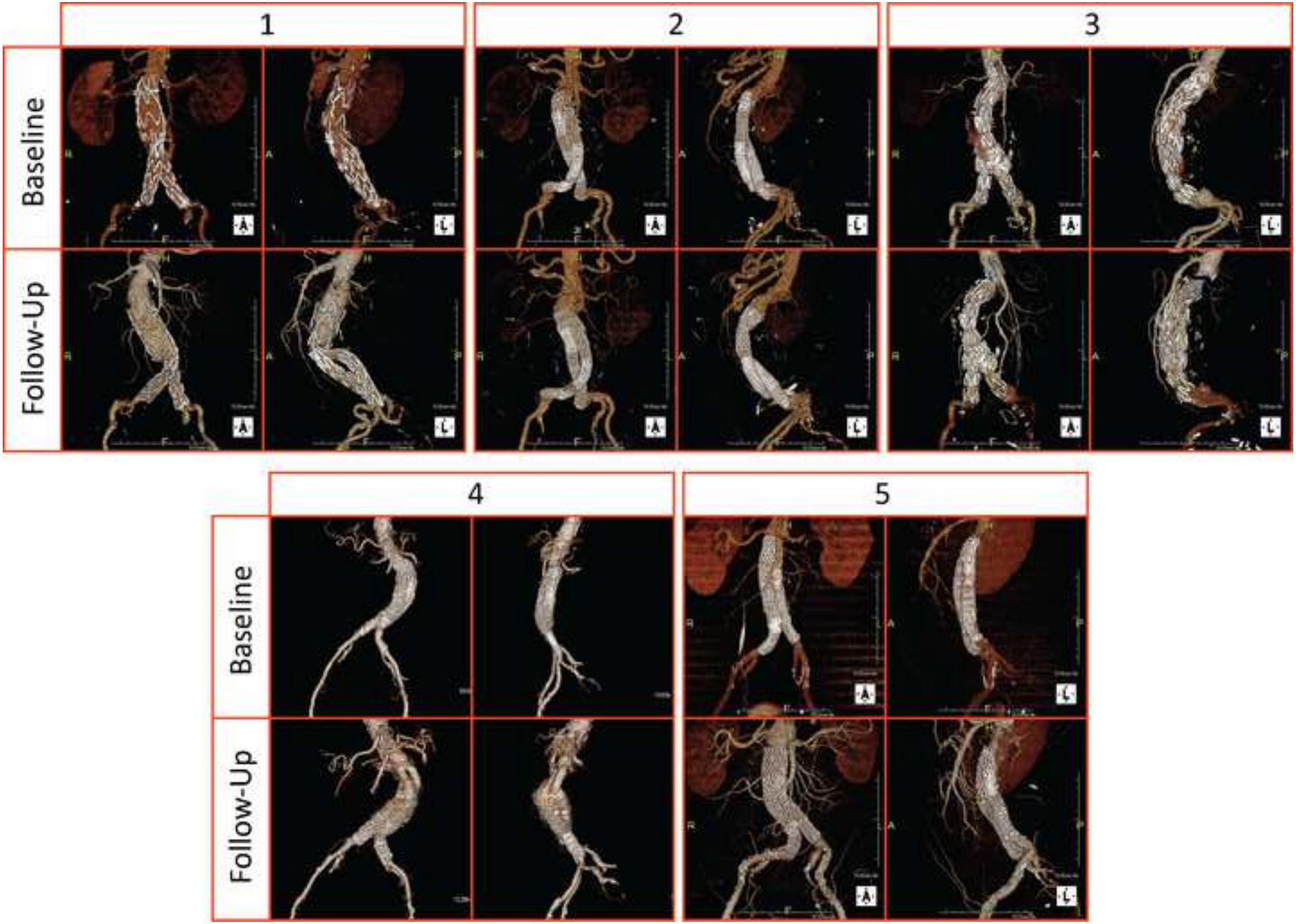

Figure 2

Click here to download high resolution image

Figure 3

Click here to download high resolution image

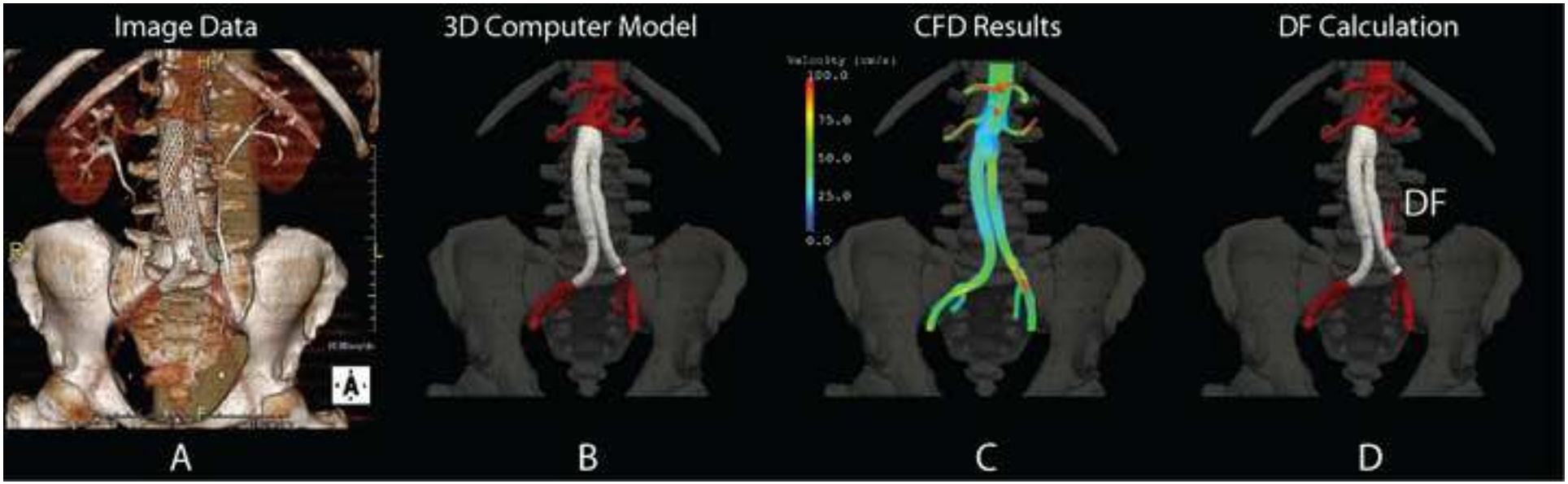

Figure 4

Click here to download high resolution image

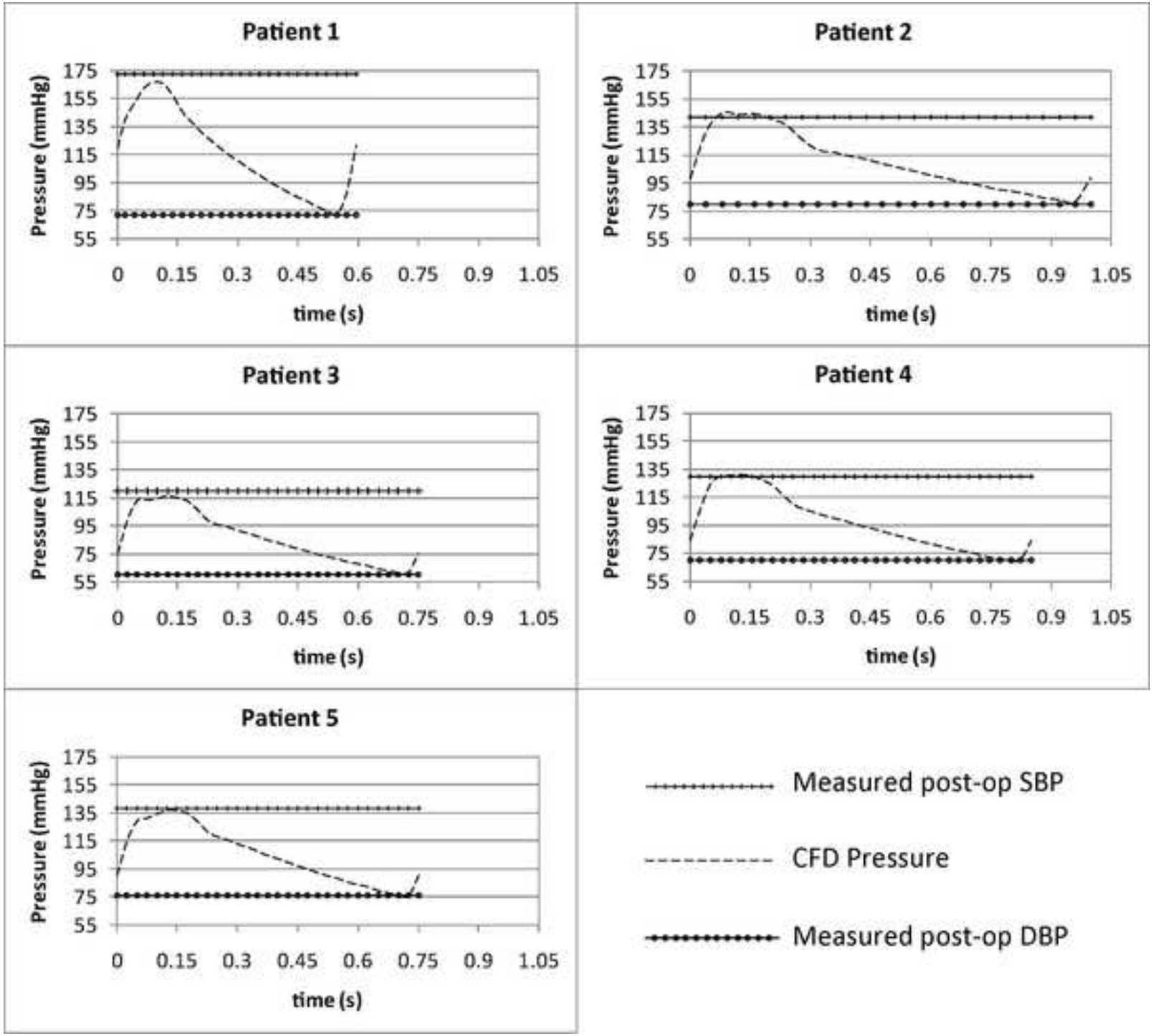

Figure 5

Click here to download high resolution image

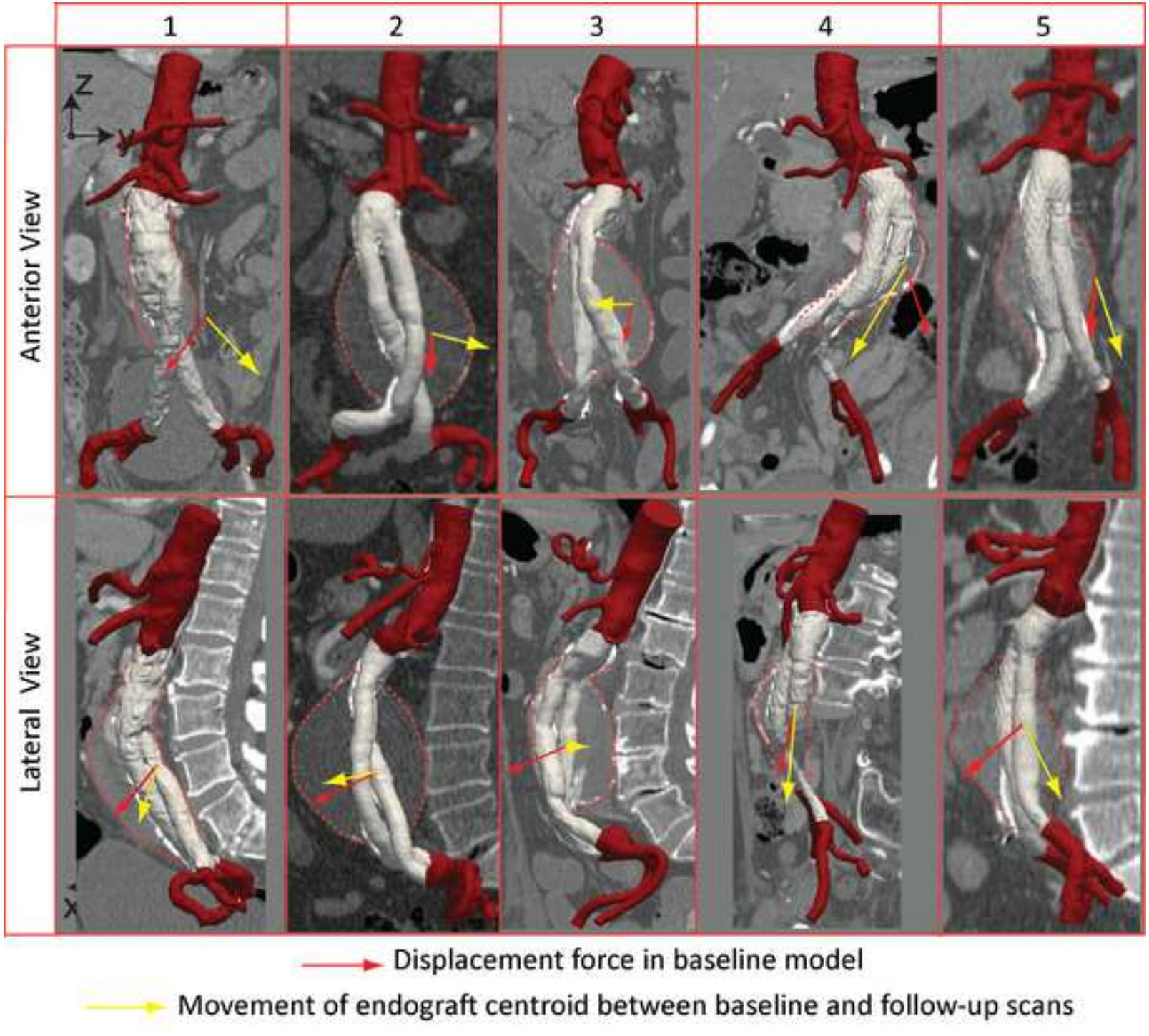

Figure/Table Legend

Figure 1: Computer Tomography data of 5 patients treated with AAA stent-grafts that experienced endograft movement. The figure shows data corresponding to the post-operative scan (baseline) and a follow-up scan usually taken just before a secondary procedure or re-intervention was performed.

Figure 2: Quantitative 3D analysis of the movement of the endograft centroid between a baseline post-operative state (top row), and a one-year follow-up state (middle row) for patient #2 of the study. The endograft centroid moves primarily in the antero-lateral direction (17.6 mm in the xy plane), and also in the axial direction (3 mm in z).

Figure 3: Computer methodology for displacement force calculation: Starting with the patient CT image data (A), 3D computer models of the endograft and the abdominal aorta are built (B). Then, CFD analyses calculating blood flow velocity and pressure in the computer model are performed (C). Lastly, the displacement force is computed using the results of the CFD analysis (D).

Figure 4: Comparison between the computed CFD pressure and the measured systolic and diastolic post-operative pressure values for each patient. The maximum relative error between the computed and measured data for the pressure pulse is less than 3% for all the patients.

Figure 5: Displacement force and endograft centroid movement vectors in the anterior and lateral views for the 5 patients considered in the study. Relative sizes of arrows reflect magnitude of the vectors.

Table 1

Patient #	1	2	3	4	5
Age	81	81	83	78	56
Sex	m	m	m	f	m
Aneurysm diameter (mm)	58	86	60	50	60
Endograft type	32 mm suprarenal	28 mm infrarenal	32 mm suprarenal	28 mm infrarenal	28 mm infrarenal
BP (mmHg)	172/72	142/80	120/60	130/70	138/76
HR (bpm)	101	60	80	70	80
Body surface area (m^2)	2.0	2.4	1.7	1.5	2.3
Estimated SC flow (L/min)	2.9	3.8	2.3	1.80	3.7
Follow-up interval	3 y	1 y	8 m	3.5 y	8.5 y
Clinical migration	Yes	Yes	Yes	Yes	No

TABLE 1

Age, sex, preoperative aneurysm diameter, endograft type, post-operative morphometric indices, follow-up interval, and occurrence of clinical migration for the 5 patients included in the study.

Table 2

Patient #	1	2	3	4	5
Movement Magnitude (mm)	**17.5**	**18.0**	**9.0**	**28.8**	**14.0**
Anterior (x) (mm)	4.0	12.1	-0.5	2.6	-6.0
Lateral (y) (mm)	11.0	13.0	-9.0	-14.5	4.0
Axial (z) (mm)	-13.0	-3.0	0.0	-24.8	-12.0
DF Magnitude (N)	**4.8**	**9.5**	**5.6**	**3.7**	**5.2**
Anterior (x) (N)	2.6	8.5	5.0	0.8	3.9
Lateral (y) (N)	-2.4	-0.4	-0.7	1.1	-0.5
Axial (N)	-3.3	-4.2	-2.3	-3.3	-3.4
Correlation Metric cos(α)	**0.31**	**0.65**	**0.08**	**0.66**	**0.20**

TABLE 2

3D movement (mm) of endograft centroid between BL and FU scans for each patient. The movement is decomposed into its anterior, lateral and axial components. 3D Displacement force DF (given in Newtons) acting on the endograft in the post-operative configuration. The DF vector is decomposed into its anterior, lateral and axial components. Correlation metric calculated as the cosine of the angle α between the post-operative DF and movement vectors for the 5 patients of the study.